Mol. Cryst. Liq. Cryst., Vol. 527: pp. 43/[199]–52/[208], 2010

ISSN: 1542-1406 print/1563-5287 online
DOI: 10.1080/15421406.2010.486622

Taylor & Francis
Taylor & Francis Group

Asymmetry Peculiarities of Surface-Mediated Liquid Crystals Gratings Recorded Due to Light-Induced Anchoring

E. OUSKOVA,[1] N. ARYASOVA,[1] V. BOICHUK,[1] D. FEDORENKO,[1] K. SLYUSARENKO,[1,2] AND YU. REZNIKOV[1]

[1]Institute of Physics, National Academy of Sciences of Ukraine, Kiev, Ukraine
[2]Laboratoire des Colloïdes, Verres et Nanomatériaux, Université Montpellier II/CNRS, Bataillon, Montpellier, France

The peculiarities of the director and polarization gratings recorded due to light-induced anchoring effect in liquid crystal media doped with azo-dye were found and studied. Depending on the ratio of the grating period to the cell's thickness, either asymmetrical LC director distribution or quasi-sinusoidal director modulation were formed. The observed behavior can be explained in terms of surface and bulk interaction of twist domains presenting the grating stripes. We showed the possibility to control the grating diffraction efficiency by applying the ac electric field, increasing the diffraction efficiency up to 30%.

Keywords Holographic gratings; light-induced anchoring; liquid crystal

Introduction

The patterning of surfaces of liquid crystals (LCs) is under tough attention to have possibility of creating the variety of hybrid geometries and multi-domain configurations for wide-angle viewing LC displays, projection displays, and photonic devices [1]. A big variety of materials and techniques were used to form complex configurations in liquid-crystal materials to get unique electro-optic behavior [2–5] compared to the well-described single-domain LC alignment typically produced with rubbing technique.

At the beginning of 90 s Gibbons *et al.*, Reznikov *et al.*, and Schadt *et al.* proposed new perspective method of alignment and pattering of LCs by light – so named photo-alignment technique [6–9]. This technique uses polarized light to induce anisotropy in a photosensitive aligning layer. The light-induced anisotropy of the irradiated layer causes appearance of the easy orientation axis $\vec{e}$ of LC director $\vec{n}$ on a photosensitive surface. Easy control of the easy axis direction and the value of the anchoring energy W by variation of the light polarization and intensity made the photoaligning effects

Address correspondence to E. Ouskova, Institute of Physics, National Academy of Sciences of Ukraine, Pr. Nauki 46, Kyiv 03039, Ukraine. Tel.: +(38044)5250779; Fax: +(38044)5250830; E-mail: ouskova@iop.kiev.ua

as a base of new advanced technology of the orientation of LCs in LCD and telecommunication industries, and gave a powerful tool for surface LC physics.

The other interesting type of photoalignment effect is bulk-mediated photoalignment discovered by Voloshchenko *et al.* in 1995 [10] and later called as a light-induced anchoring. It was found that irradiation of a nematic LC bulk doped with azo-dye by polarized light in the dye absorption band produced a robust easy orientation axis on a non-photosensitive polymer aligning surface. The experiments [11–14] showed that the effect of light-induced anchoring was governed by competition between light-induced desorption of azo-dye from spontaneously adsorbed layer of dye molecules and adsorption of dye molecules from LC bulk on the aligning surface. The light-induced desorption of dye molecules resulted in the easy axis in direction away from the polarization of the pump light, $\vec{E}$, and the light-induced adsorption caused the easy axis in direction toward $\vec{E}$. At low light irradiation doses desorption prevails, and light-induced adsorption dominates at high irradiation doses. In addition, a light-induced bulk torque results in a LC director deviation from the easy axis orientation and via light-induced adsorption/desorption processes leads to a drift of the easy axis in a nematic phase [14]. It was shown that the effect of the light-induced anchoring is extremely promising for variety of applications due to weak intensities ($\sim 1\,\mathrm{W/cm^2}$) necessary to produce an easy axis [15]. In particular, modulation of the easy orientation axis due to light-induced adsorption/desorption of azo dye on/from aligning surfaces of dye-doped LC cell can be effectively used for formation of the complex LC patterns [16]. Moreover, the sensitivity of the effect of light-induced anchoring to light polarization allows recording the polarization holograms [17–24] in a LC.

Here we report on a recording of effective surface-mediated polarization holograms in a LC cell doped with azo-dye recorded due to light-induced anchoring, revealing unusual properties due to asymmetric surface director distribution, and demonstrating an effective control the grating diffraction efficiency by LC reorientation in the cell with electric field.

Materials and Experiments

To study the gratings' recording due to light-induced anchoring we used the commercial liquid crystal pentyl-cyano-biphenyl (5CB) from Merck with clearing point $T_c = 34.5^{\circ}\mathrm{C}$, that was doped with the azo dye Methyl Red (MR) from Aldrich. in the weight concentration $c = 0.5\%$. The effect of light-induced anchoring is well investigated in this system [10–14] that simplified the optimization of the experimental parameters and analysis of the experimental results.

The polarization holographic gratings were recorded in the combined cells made from the reference and tested substrates. Both substrates were covered with indium tin oxide electrodes. The reference substrate then was covered with rubbed polyimide layer that provided a strong planar anchoring with 1.5° pretilt angle. The tested substrate then was coated with layer of fluorinated polyvinyl-cinnamate (PVCN-F). The PVCN-F film was irradiated with polarized UV light (beam intensity $I_{UV} = 5\,\mathrm{mW/cm^2}$) during 15 min using a Hg lamp. UV irradiation made the PVCN-F film stable against dissolving in LC, and induced the easy orientation axis $\vec{e}_{test}$ with zero pretilt perpendicular to the UV light polarization. The LC cells with parallel directions of the easy axes $\vec{e}_{ref}$, $\vec{e}_{test}$ were assembled with a thickness in a range of $10 \div 40\,\mu\mathrm{m}$.

The cells were filled with the LC doped with azo-dye at the temperature above the clearing point and slowly cooled down to the room temperature. During the cooling

the cell was put on a metal brick, so that the tested substrate was facing the heated brick surface. In this geometry the nematic phase in the cell nucleated at the reference surface first and extended into the LC bulk after. It resulted in a uniform planar alignment of LC over the cell parallel to the rubbing direction of the reference surface, $\vec{e}_{ref}$.

The basic experimental setup for holographic grating recording is presented in Fig. 1. The cell was placed in the intersection of two circular polarized (left and right-handed) recording beams of the equal intensities from the diode-pumped solid state laser ($\lambda = 0.532\,\mu m$, $P_{pump} \leq 100\,mW$). The cell was irradiated from the side of the tested surface and the beam's diameter in the cell's plane was about 1 mm. The wavelength $\lambda = 0.532\,\mu m$ of the laser beams corresponded to the adsorption band of the MR molecules [25, 26].

The summation of circular polarized beams $\vec{E}_{\pm} = E_0 \begin{pmatrix} 1 \\ \pm i \end{pmatrix} e^{i\left(\pm x k_0 \sin\frac{\alpha}{2} + z k_0 \cos\frac{\alpha}{2}\right)}$, here $\vec{k}_0$ is the wave vector of the pump light and $\alpha = 2\arctan\left(\frac{l}{2L}\right)$, L is a distance to the cell's plane, that is focal distance f of a lens, and l – the distance between two beams Fig. 1, provided the linearly polarized field, $\vec{E}$, spatially modulated with a wave vector $\vec{q} = \vec{e}_{ref} k_0 \sin\frac{\alpha}{2}$ in the cell's plane:

$$\vec{E}(z=0) = \vec{E}_+ + \vec{E}_- = 2E_0 \begin{pmatrix} \cos\psi \\ -\sin\psi \end{pmatrix}, \tag{1}$$

where $\psi(x) = \arctan(\tan qx)$ is saw-tooth periodical function of polarization orientation in the cell's plane, $\vec{E}$, counted from the axis $0x$ (Fig. 2).

The plane of incidence was parallel to initial direction of LC director that is grating vector $\vec{q}$, ($q = 2\pi/\Lambda$, Λ is the period of the grating) was parallel to $\vec{e}_{ref}$. The gratings' periods $\Lambda \approx \frac{\lambda L}{l}$ were in a range of $10 \div 80\,\mu m$.

Taking into account previous research on light-induced anchoring [11,14] we chose the following conditions of the experiments: incident light intensity in a cell's plane was $I_0 = 1\,W/cm^2$; exposure time – $t_{exp} = 30\,min$. The holographic gratings with different periods were recorded in the cells of different thicknesses.

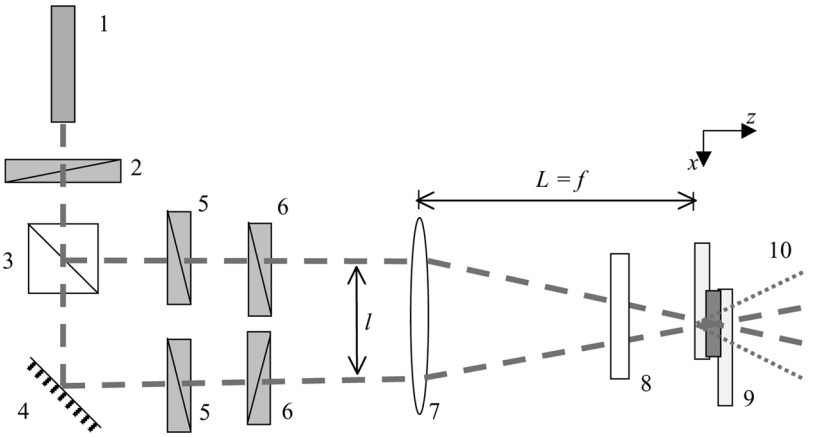

Figure 1. Experimental set-up for recording of gratings. 1 – diode-pump solid state laser, $I \leq 100\,mW$, ($\lambda = 532\,nm$; 2 – polarizer; 3 – beam-splitter cube; 4 – mirror; 5 – polarizers that make intensity of both legs equal; 6 – polarizers set at polarization -45^o and $+45^o$; 7 – lens with focal distance $f = 0.9\,m$; 8 – $\lambda/4$ waveplate; 9 – LC cell; 10 – diffracted beams.

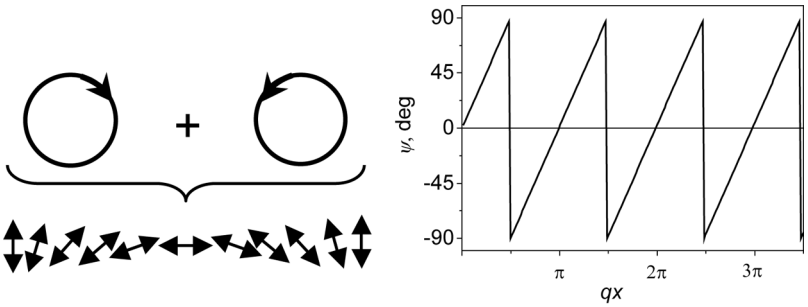

Figure 2. Interference of two circularly polarized (left and right-handed) beams (a); and spatial dependence of azimuthal angle of polarization vector in the interference plane (b).

The recorded holograms were tested by the linearly polarized light from a probe He-Ne laser ($\lambda = 0.63\,\mu m$, $P_{probe} \leq 1\,mW$). We observed the diffraction pattern on the screen behind the cell and measured the intensity of the incident and 1st order diffraction beams depending on the grating period Λ, and ac voltage ($\nu = 1\,kHz$).

The grating patterns were analyzed in the polarizing microscope equipped with the CCD-camera. Setting the polarizer along rubbing direction and rotating the analyzer from 0 to 180° with the step 10°, a set of pictures was obtained. Digital processing of these pictures allowed us to recover the spatial distribution of the director of LC in the irradiated areas. By doing this processing we suggested that all director changes occurred in azimuthal plane. i.e., only twist director deformations were produced in the cells.

Results

During the gratings' recording the self-diffraction was observed, and the amount of orders of diffraction increased with growing of grating period. The diffraction of ± 1st orders was observed at $\Lambda = 12\,\mu m$ and up to ± 13 diffraction orders were observed at $\Lambda = 50\,\mu m$. The recorded gratings were permanent and kept their characteristics

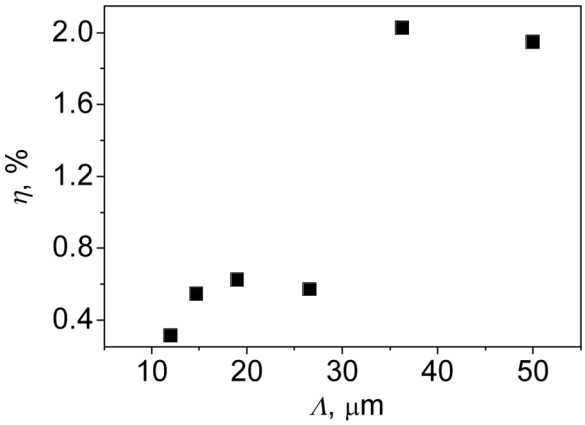

Figure 3. Dependence of diffraction efficiency η of first order diffraction on gratings' period. Cell's thickness: $d = 12\,\mu m$. Light intensity: $I = 1\,W/cm^2$. Exposure time: $t = 30\,min$.

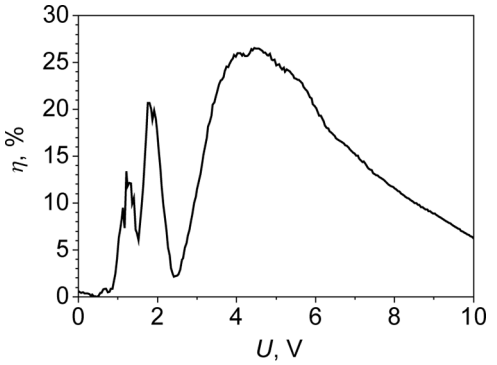

Figure 4. Dependence of diffraction efficiency η of first order diffraction on applied ac electric field (1 kHz). Cell's thickness: $d = 36\,\mu m$. Grating's period: $\Lambda = 60\,\mu m$. Light intensity: $I = 1\,W/cm^2$. Exposure time: $t = 30\,min$.

during 6 months at least. The diffraction efficiency of the gratings $\eta_{+1} = \frac{I_{d,+1}}{I_0}$ ($I_{d,+1}$ is the intensity of the $+1$ order diffraction beam) varied from 0.3 to 2 percents and increased with the period Λ (Fig. 3).

The possibility of effective controlling the grating diffraction efficiency by applying the ac electric field was found. The dependence of the diffraction efficiency η_{+1} on the voltage U is shown in Figure 4. One can see that the application of the electric field E results in the oscillating behavior of the diffraction efficiency, and

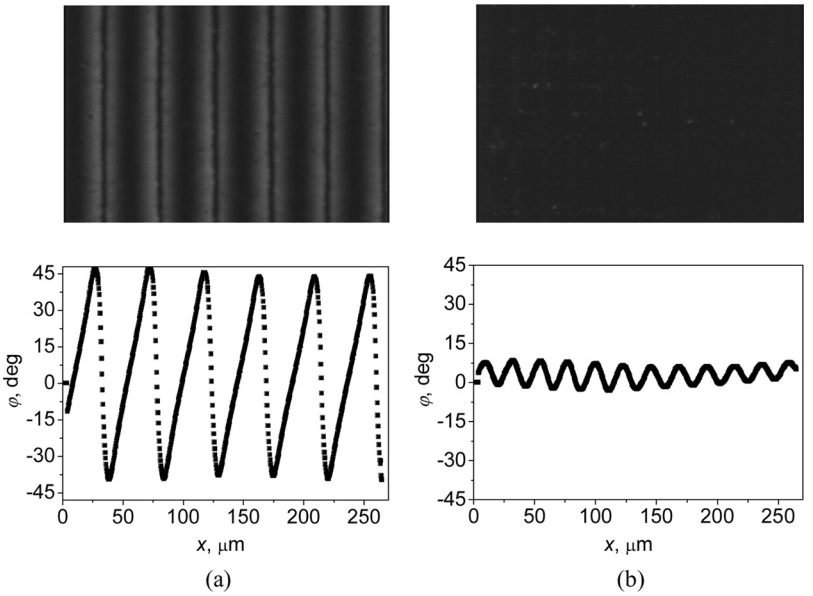

Figure 5. Holographic grating in polarizing microscope between crossed polarizers (upper row), and correspondent spatial dependence (lower row) of director twist angle through the grating period. Cell's thickness: $d = 12\,\mu m$. Light intensity: $I = 1\,W/cm^2$. Exposure time: $t = 30\,min$. Grating's period: $\Lambda = 50\,\mu m$ (a), and $19\,\mu m$ (b).

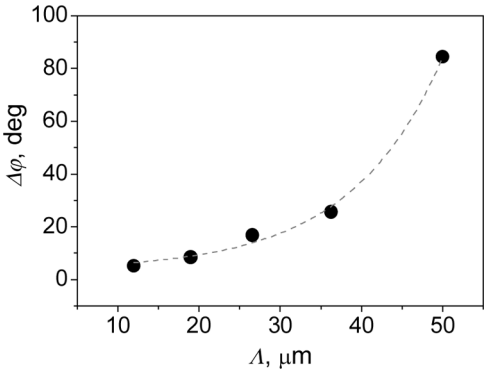

Figure 6. The dependence of average amplitude of director reorientation $\Delta\varphi$ (the average difference between maximum "+" twist angle and "−" twist angle) on grating's period. Cell's thickness: $d = 12\,\mu m$. Light intensity: $I = 1\,W/cm^2$. Exposure time: $t = 30\,min$.

in the drastic increase of the value of η_{+1}, which achieves its maximum $\eta_{+1} \approx 28\%$ at $E = 0.14\,V/\mu m$.

The observation in the polarization microscope showed the producing of the spatially modulated twist deformation in the cell. We could not unambiguously set if there was also modulation of the director in the polar plane (modulation of the pretilt). The analysis of the gratings' patterns showed different character of the director twist distribution on the tested surface, $\varphi(x)$, depending on the period of the gratings and the cell's thickness. At the large periods, $\Lambda >> d$, the spatial distribution of the director is asymmetric and has a saw-tooth shape with a thin regions of the twist sign change. The typical twist director distribution, $\varphi(x)$ of this type is presented in Figure 5a for $\Lambda = 50\,\mu m$ and $d = 12\,\mu m$. If the value Λ is comparable or less than d, the asymmetry of the director distribution $\vec{n}(x)$ disappeared and quasi-sinusoidal distribution of the twist angle occurred (Fig. 5b).

Also, the amplitude $\Delta\varphi$ of the spatial twist modulation, $\varphi(x)$, strongly depends on the period of the grating, decreasing with the decrease of Λ (Fig. 6). The remarkable fact is that the dependence $\Delta\varphi(\Lambda)$ that determines the diffraction efficiency of the gratings, does not correlate with the dependence $\eta_{+1}(\Lambda)$ (see Fig. 3), and the discrepancy between these curves is particularly manifested in the region of the transition between quasi-sinusoidal and saw-tooth director distribution.

Discussion

The observations in the polarization microscope show that the recorded holograms are the result of the light-induced spatial modulation of the director on the tested substrate in the azimuth plane $\varphi(x)$. The cause of this modulation is the effect of light-induced anchoring, which results in producing of the easy orientation axis, $\vec{e}_{test}[I_0(x), \vec{E}(x)]$ with the corresponding anchoring energy $W_{test}[I_0(x), \vec{E}(x)]$ [14]. The formation of the easy axis on the tested surface is governed by the processes of light-induced adsorption and desorption of MR molecules on/from the PVCN-F-surface in the presence of the light-induced bulk torque.

In general case after irradiation, orientations of the incident light polarization, light-induced easy axis modulated on the surface and correspondent LC director

do not coincide, and determination of these orientations is a complex problem [14,27]. We could regard that the orientation of the easy axis $\varphi(x)$ equals to the angle $\psi(x)$ plus some function $\delta(x)$ that depends on the elastic torque induced by the referent substrate, the pump light and nearby region. Because $\varphi(x)$ has a form like $\psi(x)$ with usually small deviation $\delta(x)$ [27] for the first qualitative consideration we put $\delta(x) = 0$, i.e., easy axis on the aligning surface also has a saw-shaped modulation (see (1)). We also neglected by possible spatial modulation of the anchoring energy on the tested surface.

Thus, we consider the distribution of the director in the combined cell, in which the easy axis on the tested surface is periodically modulated along the axis $0x$, according to (1) while the reference surface provides planar uniaxial orientation of the director. In order to simulate the equilibrium director field in the cell, we build a regular lattice model where the investigated surface is represented as a set of micro-domains of equal shape and area A. Each domain is much smaller than a characteristic scale of the director deformation and is denoted with a two-dimensional index $\mathbf{m} = \{m_1, m_2\}$ that defines its position $\boldsymbol{\rho}_\mathbf{m} = m_1\mathbf{a}_1 + m_2\mathbf{a}_2$, where $\mathbf{a}_1$ and $\mathbf{a}_2$ are the basic vectors of the lattice. The director field is described by the director azimuthal angles $\phi_\mathbf{m}$ at the $N_1 \times N_2$ set of micro-domains with periodic boundary conditions $\phi_{\mathbf{m}+\mathbf{M}} = \phi_\mathbf{m}$, where $\mathbf{M} = \{n_1N_1, n_2N_2\}$, n_1 and n_2 are arbitrary integers.

The equilibrium values of $\phi_\mathbf{m}$ was found by minimization of lattice free energy F that we represent as a sum of micro-domain 'energies' $E_\mathbf{m}$ and interactions between domains $J_{\mathbf{mm}'}$:

$$F = \sum_{\mathbf{m}} E_\mathbf{m} + \frac{1}{2}\sum_{\mathbf{m},\mathbf{m}}{}' J_{\mathbf{mm}'}. \tag{2}$$

The micro-domain energy $E_\mathbf{m}$ contains the surface anchoring energy (we use the Rapini-Papoular approximation) and the energy of twist deformation caused by the reference surface:

$$E_\mathbf{m} = \frac{A}{2}\left[W_\mathbf{m}\sin^2(\phi_\mathbf{m} - \psi_\mathbf{m}) + \frac{K_{22}}{d}\phi_\mathbf{m}^2\right], \tag{3}$$

where K_{22} – elastic constant, $\psi_\mathbf{m}$ and $W_\mathbf{m}$ are the azimuthal angle of the easy axis and the azimuthal anchoring coefficient of the domain $\mathbf{m}$, respectively.

We choose the potential of the interaction between micro-domains, $J_{\mathbf{mm}'}$, that corresponded to the bulk elastic energy in the cell with homogeneous and inhomogeneous substrates in the form:

$$J_{\mathbf{mm}'} = \frac{K_{eff}A^2}{4\pi|\rho_\mathbf{m} - \rho_{\mathbf{m}'}|^3}(\varphi_\mathbf{m} - \varphi_{\mathbf{m}'})^2, \tag{4}$$

where K_{eff} is effective elastic constant. The interaction between micro-domains at distances exceeding the cell thickness is screened by the interaction of each domain with the reference surface. Therefore, we also assumed that the micro-domains interact only on the distance $|\rho_\mathbf{m} - \rho_{\mathbf{m}'}|$, which is less than the critical radius $R_c \approx L$.

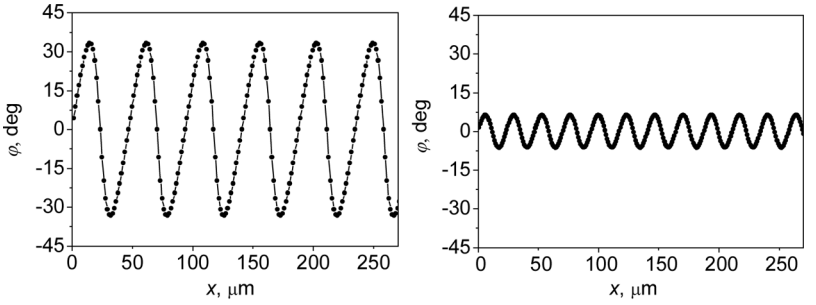

Figure 7. Simulated equilibrium director field in the cell 12 μm thick for grating period: (a) $\Lambda = 50\,\mu m$; and (b) $\Lambda = 19\,\mu m$.

The results of the calculations according to the described model have demonstrated significant dependence of the equilibrium director field on the ratio of the cell's thickness and grating period. For grating periods being much larger than the cell's thickness $\Lambda >> d$ the director field retained asymmetrical, saw-tooth shape imposed by the easy axis modulation, while for $\Lambda \leq d$ grating periods this asymmetry almost vanished and director manifested quasi-sinusoidal modulation. Figure 7 presents simulated equilibrium director field for the actual parameters of the cells used in the experiment: (a) $\Lambda = 50\,\mu m$ and $d = 12\,\mu m$; and (b) $\Lambda = 19\,\mu m$ and $d = 12\,\mu m$. As it was found experimentally (see Fig. 5), for $\Lambda = 50\,\mu m >> d$, the spatial distribution of the director is asymmetric and has a saw-tooth shape with thin regions of the twist sign change, while for $\Lambda = 19\,\mu m$ comparable with the cell thickness no asymmetry of the director distribution is found, and twist angle manifests quasi-sinusoidal spatial modulation.

The observed dependence the director distribution in the cell on the ratio of the cell thickness and grating period is caused by a competition between the surface and volume contributions to the total free energy (3). While the surface term imposes the director modulation that coincides with the saw-shaped distribution of the easy axis, the bulk term in (2) "smoothes" this distribution due to orientational elasticity of a LC. As the result of this competition, a first sinusoidal harmonic of the saw-shaped director distribution dominates at $\Lambda \leq d$.

The polarization and intensity peculiarities of the diffraction on the asymmetrical gratings deserve detailed additional studies, which are on the run. Our preliminary observations showed that the transition from the asymmetrical director distribution $\vec{n}_{test}(x)$ to the symmetrical one causes a jump of the value of the diffraction efficiency on the dependence $\eta_{+1}(\Lambda)$ around $\Lambda \approx 30\,\mu m$ (Fig. 3).

Conclusion

The peculiarities of the director and polarization gratings recorded due to light-induced anchoring effect in liquid crystal media doped with azo-dye were found and studied. Depending on the ratio of the grating period to the cell's thickness, either asymmetrical LC director distribution or quasi-sinusoidal director modulations were formed. The observed behavior can be explained in terms of surface

and bulk interaction of twist domains presenting the grating stripes. We showed the possibility to control the grating diffraction efficiency by applying the ac electric field, increasing the diffraction efficiency up to 30%.

Acknowledgments

We would like to thank V. Reshetnyak, Yu. Kurioz, S. Subota, M. Soskin, V. Slyusar. The work was partially supported by STCU project No. 4687.

References

[1] Crawford, G. P., Eakin, J. N., Radcliffe, M. D., Callan-Jones, A., & Pelcovits, R. A. (2005). *Jour. Appl. Phys.*, *98*, 123102.
[2] Song, L., Lee, W.-K., & Wang, X. (2006). *Optics Express*, *14*(6), 2197.
[3] Nersisyan, S. R., Tabiryan, N. V., Hoke, L., Steeves, D. M., & Kimball, B. (2009). *Optics Express*, *17*(3), 1817.
[4] Blinov, L. M., Cipparrone, G., Mazzulla, A., Provenzano, C., Palto, S. P., Barnik, M. I., Arbuzov, A. V., & Umanskii, B. A. (2006). *Mol. Cryst. Liq. Cryst.*, *449*, 147–160.
[5] Residori, S., Russo, G., McConville, S., & Petrosyan, A. (2005). *Mol. Cryst. Liq. Cryst.*, *429*, 111–132.
[6] Gibbons, W., Shannon, P., Sun, S.-T., & Swetlin, B. (1991). *Nature*, *49*, 351.
[7] Dyadyusha, A., Kozenkov, V., Marusii, T., Reznikov, Yu., Reshetnyak, V., & Khizhnyak, A. (1991). *Ukr. Phys. Journ.*, *36*, 1059.
[8] Schadt, M., Schmitt, K., Kozenkov, V., & Chigrinov, V. (1992). *Jpn. J. App. Phys.*, *31*, 2155.
[9] Marusii, T., & Reznikov, Yu. (1993). *Mol. Mat.*, *3*, 161.
[10] Voloshchenko, D., Khyzhnyak, A., Reznikov, Yu., & Reshetnyak, V. (1995). *Jpn. J. Appl. Phys.*, *34*, Part 1, 566.
[11] Fedorenko, D., Ouskova, E., Reshetnyak, V., & Reznikov, Yu. (2006). *Phys. Rev. E*, *73*(3), 031701.
[12] Ouskova, E., Fedorenko, D., Reznikov, Yu., Shiyanovskii, S. V., Su, L., West, J. L., Kuksenok, O. V., Francescangeli, O., & Simoni, F. (2001). *Phys. Rev. E*, *63*, 021701.
[13] Ouskova, E., Reznikov, Yu., Shiyanovskii, S. V., Su, L., West, J. L., Kuksenok, O. V., Francescangeli, O., & Simoni, F. (2001). *Phys. Rev. E*, *64*, 051709.
[14] Fedorenko, D., Slyusarenko, K., Ouskova, E., Reshetnyak, V., Ha, K.-R., Karapinar, R., & Reznikov, Yu. (2008). *Phys. Rev. E*, *77*, 061705.
[15] Simoni, F., Francescangeli, O., Reznikov, Yu., & Slussarenko, S. (1997). *Optics Lett.*, *22*(8), 549.
[16] Slussarenko, S., Francescangeli, O., Simoni, F., & Reznikov, Y. (1997). *Appl. Phys. Lett.*, *71*(25), 3613.
[17] Blinov, L. M., Barberi, R., Ciuchi, F., de Santo, M. P., Cipparrone, G., Mazzulla, A., Palto, S. P., & Yudin, S. G. (2003). *J. Nonlinear. Opt. Phys. Mater.*, *12*(4), 1–17.
[18] Blinov, L. M., Cipparrone, G., Mazzulla, A., Provenzano, C., Palto, S. P, Barnik, M. I., Arbuzov, A. V., & Umanskii, B. A. (2005). *Appl. Phys. Lett.*, *87*, 1.
[19] Cipparrone, G., Mazzulla, A., & Blinov, L. M. (2002). *J. Opt. Soc. Am. B*, *19*(5), 1157.
[20] Ono, H., Emoto, A., Kawatsuki, N., & Hasegawa, T. (2003). *Optics Express*, *11*(19), 2379.
[21] Gorkhali, S. P., Cloutier, S. G., Crawford, G. P., Pelcovits, R. A. (2006). *Appl. Phys. Lett.*, *88*, 251113.
[22] Escuti, M. J., & Jones, W. M. (2006). *Proc. of SPIE*, *6332*, 63320M.
[23] Komanduri, R. K., & Escuti, M. J. (2007). *Phys. Rev. E*, *76*(2), 021701.

[24] Komanduri, R. K., Jones, W. M., Oh, C., & Escuti, M. J. (2007). *Journ. of the SID*, *15*(8), 589–594.
[25] Lee, G. J., Kim, D., & Lee, M. (1995). *Appl. Opt.*, *34*, 138.
[26] Delaire, J. A., & Nakatani, K. (2000). *Chem. Rev.* (Washington, D.C.) *100*, 1817.
[27] Fedorenko, D., Ouskova, E., Reshetnyak, V., Reznikov, Yu., Lucchetti, L., & Simoni, F. (2004). *Mol. Cryst. Liq. Cryst.*, *421*, 235–242.